Signal Reconstruction with Generalized Sampling

Yamamoto, Kaoru
Automatic Control LTH, Lund University

Nagahara, Masaaki
Institute of Environmental Science and Technology, The University of Kitakyushu

Yamamoto, Yutaka
Kyoto University : Professor Emeritus

出版情報：2017 IEEE 56th Annual Conference on Decision and Control (CDC), pp.6253-6258, 2017. Institute of Electrical and Electronics Engineers (IEEE)
バージョン：
権利関係：

Signal Reconstruction with Generalized Sampling

Kaoru Yamamoto[1], Masaaki Nagahara[2], and Yutaka Yamamoto[3]

***Abstract*— This paper studies the problem of reconstructing continuous-time signals from discrete-time uniformly sampled data. This signal reconstruction problem has been studied by the authors in various contexts, and led to a new signal processing paradigm. The crux there is to employ a physically realizable signal generator model, and design an (sub)optimal filter via $H^\infty(\mathbb{C}_+)$ optimal sampled-data control theory. The present paper extends this framework to the situation where sampling is more general having a generalized sampling kernel. It is more consistent with a more general framework, for example, wavelet signal expansion, and can lead to a more general applications. We give a general setup along with a solution via fast-sample/fast-hold approximation. A simulation is presented to illustrate the result.**

I. Introduction

A central problem in digital signal processing is that of reconstructing the original analog signal from its sampled data. When sampling is uniform and ideally performed, i.e., reading out the sampled values precisely at sampled points, the celebrated sampling theorem, e.g., [13], gives a perfect answer *as long as the frequency contents are strictly band-limited below the Nyquist frequency* π/h [rad/sec], where h is the underlying sampling period. Based on this perfect band-limiting assumption, Shannon [6] proposed his signal processing paradigm. In spite of various drawbacks such as non-causal construction, slow convergence, etc., this paradigm has dominated digital signal reconstruction until today.

In contrast to such developments, the present authors have developed and proposed a completely new methodology based on H^∞ sampled-data control theory: [12], [4], [5].

The central idea there is quite different from that of the Shannon paradigm in that it does not assume perfect band-limiting hypothesis on the original signals to be reconstructed. Instead, we assume that the signal class obeys a certain decay curve in its frequency energy distribution that is governed by a linear finite-dimensional system. This is a much more realistic assumption in that in many signals produced by physical devices, e.g., musical instruments, there is always a signal generator and associated signal models, and they mostly obey a certain frequency decay curve induced by such a model.

This new method has been applied to sound and image processing, and has proven quite successful [8], [11]. In particular, it is implemented in a sound-processing LSI chips, whose cumulative production has reached over 65 million chips.

In these applications, however, sampling is still limited to be ideal, that is, we assume instantaneous signal values $\{f(nh)\}_{n=0}^{\infty}$ for a signal f. There are two representative cases where we want to consider non-ideal sampling actions. First, in reality, sampling is usually conducted by integrating signals with a certain kernel function. Any physical sensing devices are always accompanied with such an integration, and pure ideal sampling is a limit of such a process. Another notable and important situation is that of wavelet expansion where we expand functions in terms of scaling or wavelet functions. Expansion coefficients are obtained through the inner product with a scaling or wavelet function, and we again encounter a sampling process with integration.

In order to circumvent the limitation of ideal sampling and expand the applicability of the method developed in [12] etc., this paper studies the signal reconstruction problem with such a generalized sampling induced by integration with a kernel function.

While the framework in [12] is basically compatible with the current wavelet analysis, there also arise some technical issues that require a careful generalization. For example, the Daubechies scaling function ${}_2\phi$ ([2]) has support in $[0, 3h]$. This means that in order to compute the values of the generalized sampling, one has to hold the input function for 3 sampling periods, and take the inner product of the signal with the kernel function with 3 steps of delay. The lifting technique [1], [9] gives a transparent formulation of this setting. We then modify the design method developed in [12] to the present context to obtain an optimal filter. The detail of the precise problem formulation is given in the subsequent section.

This method has an added advantage: In practice, we generally do not have real continuous-time data but only sampled values, ideal or non-ideal. This makes it difficult to apply standard wavelet expansion analysis due to the lack of information with higher resolution (referred to as a *wavelet crime* in [7]). The present method can be used to optimally interpolate the intersample behavior yielding the lost information in detail. The objective here is then to reconstruct the original analog signal including the intersample behavior (sub)optimally in the sense of H^∞. Then one obtains an optimal reconstruction including the intersample

[1]Automatic Control LTH, Lund University, Box 118, SE 221 00 Lund, Sweden; this author is a member of the LCCC Linnaeus Center and the ELLIIT Excellence Center at Lund University. k.yamamoto@ieee.org.

[2] Institute of Environmental Science and Technology, The University of Kitakyushu, Fukuoka 808-0135, Japan. nagahara@ieee.org.

[3]Professor Emeritus, Kyoto University, Kyoto 606-8510, Japan yy@i.kyoto-u.ac.jp. This work was supported in part by the Japan Society for the Promotion of Science under Grants-in-Aid for Scientific Research No. 15H04021 and 24360163. The author wishes to thank DIGITEO and Laboratoire des Signaux et Systemes (L2S, UMR CNRS), CNRS-CentraleSupelec-University Paris-Sud and Inria Saclay for their financial support while part of this research was conducted.

behavior, enabling a higher-order expansion. The overall analog information is controlled by a high-frequency decay rate peculiar to the signal generator we consider. The detail will be described below.

The paper is organized as follows: Section II gives the basic signal reconstruction formulation. The difficulty here is that the generalized sampling induces a certain amount of delays, and this requires further modifications in the design formulas. This will be discussed in the subsequent two sections. We give formulas for design via the fast-sample/fast-hold approximation in Section III. A design example is given in Section IV using the Daubechies 2 scaling function. Aside from the fact that this treatment is new in this context, we also see that while for the bare expansion it gives a rather poor approximation result, it will be substantially improved by introducing upsampling and corresponding filter design. Concluding remarks are given to indicate issues for future study in Section V.

II. Problem formulation

Consider the sampled-data system depicted in Fig. 1.

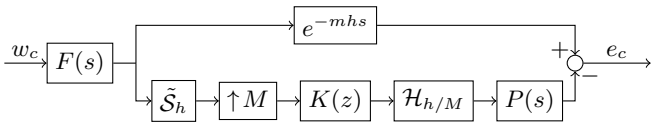

Fig. 1: Signal reconstruction error system

The exogenous signal w_c goes through a linear time-invariant system $F(s)$, and becomes band-limited to become the actual target analog signal y. This $F(s)$ models the physical characteristic of the signal generator, e.g., a musical instrument, and governs the decay rate of high frequency in the signal y. The totality of such y constitutes the signal class to be reconstructed. We take F to be rational and strictly proper so that the resulting filter has a low-pass characteristic. The filtered y is then processed by the generalized sampler $\tilde{\mathcal{S}}_h$ whose definition is given as follows:

$$(\tilde{\mathcal{S}}_h(y))[k] := \int_0^{Lh} \phi(t)y(kh+t)dt \qquad (1)$$
$$= \sum_{i=0}^{L-1} \int_{ih}^{(i+1)h} \phi(t)y(kh+t)dt,$$

where the kernel function ϕ is assumed to have support in $[0, Lh]$. In the case of the Haar scaling function $L = 1$, but for many applications, L is greater than 1. For example, Daubechies N scaling function, $L = 2N - 1$; likewise for other wavelet or scaling functions. Hence we must allow step L delays to obtain the actual sampled values $y_d[k]$, $k = 0, 1, 2 \ldots$. This is what is defined in (1).

Figure 2 (left) shows an example of the sampling kernel $\phi(t)$.

The discrete-time signal y_d is first upsampled by by factor M by the upsampler $\uparrow M$:

$$\uparrow M : y_d \mapsto x_d : x_d[k] = \begin{cases} y_d[l], & k = Ml,\ l = 0, 1, \ldots \\ 0, & \text{otherwise} \end{cases},$$

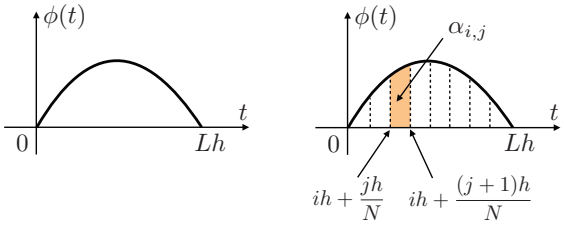

Fig. 2: Sampling kernel $\phi(t)$ (left) and fast discretization of $\phi(t)$ (right)

and becomes another discrete-time signal x_d with sampling period h/M. The discrete-time signal x_d is then processed by a digital filter $K(z)$ to be designed, and becomes a continuous-time signal u_c by going through the zero-order hold $\mathcal{H}_{h/M}$ (which works in sampling period h/M), and then becomes the final signal z_c by passing through an analog buffer filter $P(s)$. Here $P(s)$ can be assumed to be 1 for simplicity. An advantage here is that one can use the fast hold device $\mathcal{H}_{h/M}$ thereby making possible more precise signal restoration. The objective here is to design a digital filter $K(z)$ for a given $F(s)$, M and $P(s)$, to optimally reconstruct the filtered signal y.

Fig. 1 shows the block diagram for the error system for the design. The delay in the upper portion of the diagram corresponds to the fact that we allow a certain amount of time delay for signal reconstruction. Let T_{ew} denotes the input/output operator from w_c to $e_c(t) := y(t-mh) - z_c(t)$. Our design objective is as follows:

Problem 1: Given stable $F(s)$ and $P(s)$ and an attenuation level $\gamma > 0$, find a digital filter $K(z)$ such that

$$\|T_{ew}\|_\infty = \sup_{w_c \in L^2[0,\infty)} \frac{\|T_{ew} w_c\|_2}{\|w_c\|_2} < \gamma.$$

Remark 2.1: The above L^2-induced norm $\|T_{ew}\|_\infty$ is indeed the H^∞-norm of the operator T_{ew} [10].

III. Solution Method via Fast-sample/fast-hold approximation

The system given by Figure 1 can be cast into a single-rate sampled-data system via lifting [1], [9], and the H^∞ control problem can be solved. Particularly, it is practical to employ the fast-sample/fast-hold approximation to obtain an approximate solution. The details can be found in [12].

However, there is an extra issue here. Since the generalized sampler (1) induces an extra delay term in obtaining sampled values, we must derive the formula for the fast discretization of $\tilde{\mathcal{S}}_h$.

Let us first discretize the sampling intervals $[0, h), [h, 2h), \ldots$ with the fast sampling grid $\{0, h/N, 2h/N, \ldots, (N-1)h/N\}$, $\{h, h + h/N, h + 2h/N, \ldots, h + (N-1)h/N\}$, etc. See Figure 2 (right) for the fast sampling approximation of ϕ. Then Figure 3 shows the block diagram for the fast discretization on these grids to obtain the operator $S = \tilde{\mathcal{S}}_h \mathcal{H}_{h/N}$.

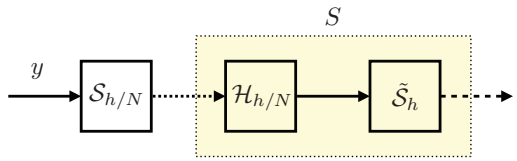

Fig. 3: Fast discretization S of $\tilde{\mathcal{S}}_h$

According to this figure, we have

$$\begin{aligned} y_d[k] &= \tilde{\mathcal{S}}_h(y) \\ &= \sum_{i=0}^{L-1} \int_{ih}^{(i+1)h} \phi(t) y(kh+t) dt \\ &= \sum_{i=0}^{L-1} \sum_{j=0}^{N-1} \int_{ih+jh/N}^{ih+(j+1)h/N} \phi(t) y(kh+t) dt \\ &= \sum_{i=0}^{L-1} \sum_{j=0}^{N-1} y(kh+ih+jh/N) \underbrace{\int_{ih+jh/N}^{ih+(j+1)h/N} \phi(t) dt}_{=:\alpha_{i,j}} \\ &= \sum_{i=0}^{L-1} \begin{bmatrix} \alpha_{i,0} & \alpha_{i,1} & \dots & \alpha_{i,N-1} \end{bmatrix} \tilde{y}_i[k], \end{aligned}$$

where $\alpha_{i,j}$ is defined as

$$\alpha_{i,j} := \int_{ih+jh/N}^{ih+(j+1)h/N} \phi(t) dt \tag{2}$$

and $\tilde{y}_i[k]$ as

$$\tilde{y}_i[k] := \begin{bmatrix} y(kh+ih) \\ y(kh+ih+h/N) \\ \vdots \\ y(kh+ih+(N-1)h/N) \end{bmatrix}.$$

See Figure 2 (right) for $\alpha_{i,j}$. We assume (2) can be easily computed. For example, by using the trapezoidal rule, we can numerically compute $\alpha_{i,j}$ by

$$\alpha_{i,j} = \frac{\phi(ih+jh/N) + \phi(ih+(j+1)h/N)}{2} \cdot \frac{h}{N}$$

Summarizing, we have the fast discretization of generalized sampler $\tilde{\mathcal{S}}_h$ given by the matrix

$$S_i = \begin{bmatrix} \alpha_{i,0} & \alpha_{i,1} & \dots & \alpha_{i,N-1} \end{bmatrix}.$$

Finally, we have

$$y_d[k] = \sum_{i=0}^{L-1} S_i \tilde{y}_i[k].$$

Figure 4 shows the block diagram of the discretized operator S for $L = 3$ in Figure 3. Here $\mathbb{L}_N$ is the discrete-time lifting by down-sampling ratio N defined by

$$\mathbb{L}_N := (\downarrow N) \begin{bmatrix} 1 \\ z \\ \vdots \\ z^{N-1} \end{bmatrix}$$

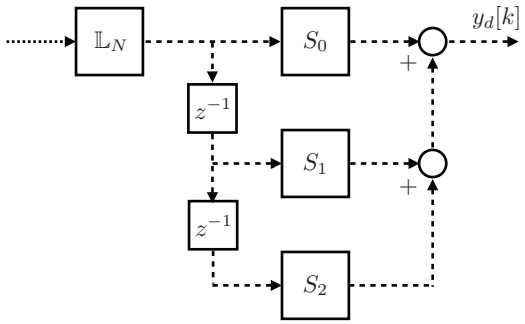

Fig. 4: Realization of fast discretization S for $L = 3$

where $(\downarrow N)$ denotes the downsampler

$$\downarrow N : x_d \mapsto y_d : y_d[k] = x_d[Nk].$$

We are now ready to employ the fast sample/hold approximation to solve the H^∞ control problem. For brevity of notation, we adopt the following shorthand notation for the transfer function $D + C(zI - A)^{-1}B$:

$$\left[\begin{array}{c|c} A & B \\ \hline C & D \end{array}\right] := D + C(zI - A)^{-1}B.$$

Consider the generalized plant shown in Figure 5. The filter $\tilde{K}(z)$ is an LTI (linear and time-invariant), single-input /M-output system. Introducing the inverse discrete time lifting by upsampling ratio M as

$$\mathbb{L}_M^{-1} := \begin{bmatrix} 1 & z^{-1} & \dots & z^{-M+1} \end{bmatrix} (\uparrow M),$$

$\tilde{K}(z)$ can be written as

$$\begin{aligned} \tilde{K}(z) &= \mathbb{L}_M K(z) (\uparrow M) \\ &= \mathbb{L}_M K(z) \mathbb{L}_M^{-1} [1 \ 0 \ \dots \ 0]^T. \end{aligned}$$

The sampled-data error system T_{ew} can be approximated by a discrete-time LTI system as in the following theorem.

Theorem 1: Let state-space realizations of $F(s)$, $P(s)$ and $K(z)$ be given by

$$F(s) = \left[\begin{array}{c|c} A_{F_c} & B_{F_c} \\ \hline C_{F_c} & D_{F_c} \end{array}\right], \quad P(s) = \left[\begin{array}{c|c} A_{P_c} & B_{P_c} \\ \hline C_{P_c} & D_{P_c} \end{array}\right],$$
$$K(z) = \left[\begin{array}{c|c} A_K & B_K \\ \hline C_K & D_K \end{array}\right].$$

Let $N = Ml$ where l is a positive integer, and define the discrete-time LTI system T_N as follows:

$$T_N(z) = z^{-m} F_N(z) - P_N(z) H \widetilde{K}(z) S(z) F_N(z),$$

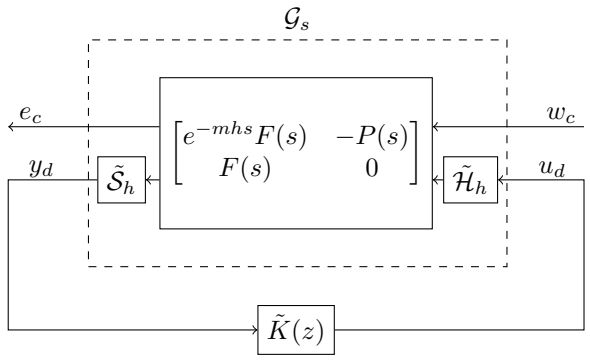

Fig. 5: Sampled-data control system

where

$$F_N = \left[\begin{array}{c|ccc} A_F^N & A_F^{N-1}B_F & A_F^{N-2}B_F & \dots & B_F \\ \hline C_F & 0 & 0 & \dots & 0 \\ C_FA_F & C_FB_F & 0 & \ddots & \vdots \\ \vdots & \vdots & \vdots & \ddots & 0 \\ C_FA_F^{N-1} & C_FA_F^{N-2}B_F & C_FA_F^{N-3}B_F & \dots & 0 \end{array}\right],$$

$$P_N = \left[\begin{array}{c|ccc} A_P^N & A_P^{N-1}B_P & A_P^{N-2}B_P & \dots & B_P \\ \hline C_P & D_P & 0 & \dots & 0 \\ C_PA_P & C_PB_P & D_P & \ddots & \vdots \\ \vdots & \vdots & \vdots & \ddots & 0 \\ C_PA_P^{N-1} & C_PA_P^{N-2}B_P & C_PA_P^{N-3}B_P & \dots & D_P \end{array}\right],$$

$$\tilde{K}(z) = \left[\begin{array}{c|c} A_K^M & A_K^{M-1}B_K \\ \hline C_K & D_K \\ C_KA_K & C_KB_K \\ \vdots & \vdots \\ C_KA_K^{M-1} & C_KA_K^{M-2}B_K \end{array}\right],$$

$$A_F = e^{A_{F_c}h/N}, \quad B_F = \int_0^{h/N} e^{A_{F_c}t}B_{F_c}\, dt,$$

$$A_P = e^{A_{P_c}h/N}, \quad B_P = \int_0^{h/N} e^{A_{P_c}t}B_{P_c}\, dt,$$

$$H := \mathrm{diag}\,\{I_l\} \in \mathbb{R}^{N\times M},\ I_l := [1,1,\dots,1]^T \in \mathbb{R}^l,$$

$$S(z) := \sum_{i=0}^{L-1} z^{-i}S_i \in \mathbb{R}^{1\times N}.$$

Then, for each fixed $\widetilde{K}$ and for each $\omega \in [0, 2\pi/h)$, the frequency response

$$\|T_N(e^{j\omega h})\| \to \|T_{ew}(e^{j\omega h})\|,$$

as $N \to \infty$, and this convergence is uniform with respect to $\omega \in [0, 2\pi/h)$. Furthermore, this convergence is also uniform in $\widetilde{K}$ if $\widetilde{K}$ ranges over a compact set of filters.
The proof is almost the same as in [12, Theorem 1].

IV. Design example

In this section we demonstrate the effectiveness of the present framework via two numerical examples.

Example 4.1: We design the filter $K(z)$ with upsampling factor $M = 8$, sampling period $h = 1$, and delay step $m = 4$. As the kernel function for the generalized sampling, we employ the Daubechies 2-scaling function ${}_2\phi$; hence $L = 3$. We take the analog filters $F(s)$ and $P(s)$ as

$$F(s) = \frac{1}{(Ts+1)(0.1Ts+1)},\ T = 7.0187,\ P(s) = 1.$$

Reflecting a typical energy distribution of orchestral music, the time constant $T = 7.0187$ is taken to be equivalent to 1 kHz with sampling frequency 44.1 kHz, under normalization of $h = 1$. The filter $F(s)$ corresponds to an energy distribution that decays by -20 dB per decade from 1 kHz and -40 dB per decade from 10 kHz.

The simulation results are shown in Figures 6a – c.

Figure 6a shows the response of the designed filter against the input $\sin(\pi/8)t$. This is below the Nyquist frequency π, and the response shows a good tracking performance. (The original sinusoid is delayed to accommodate the delay induced by the sampling and reconstruction process.) However, comparing this with Figure 7a, we see that the advantage of the current framework where the approximation is quite poor without upsampling.

This is still for tracking in low frequency. In order to really ensure the approximation quality of the present method, we show the response against a signal that contains components above the Nyquist frequency. This is not very adequate for the conventional Shannon paradigm where the reconstruction is limited below the Nyquist frequency. Figure 6b shows the response against the input signal $\sin(\pi/8)t + 0.05\sin(9\pi/8)t$. This result shows tracking to this signal with such a high-frequency component. Although this shows a fairly good tracking, its non-upsampled counterpart Figure 7b gives a very poor tracking performance, almost indistinguishable from the one shown in Figure 7a, ignoring the high-frequency component $0.05\sin(9\pi/8)t$. This clearly exhibits the advantage of the present framework allowing the intersample interpolation with upsampler and signal generator $F(s)$.

Figures 6c and 7c also further show the tracking results for $\sin(\pi/8)t$ with phase-shifted $0.05\sin((9\pi/8)t + 10)$. Again the upsampled result Figure 6c shows a better result compared to Figure 7c. (Note that we have shifted the response due to the delay e^{-mhs}, to make the comparison clearer.)

On the other hand, the present generalized sampling, particularly with a continuous kernel, does not necessarily work well for discontinuous signals or signals with much high frequency. For example, the Daubechies kernels do not work well for some discontinuous functions like rectangular waves. This is not surprising since such kernel functions were developed to allow for more efficient expansion for continuous or smooth signals. The following example gives some ideas.

Example 4.2: Figure 8 shows their responses against a rectangular wave. The filters are designed with the same $F(s)$ as Example 4.1, but here we take $h = 0.1$ and $M = 2$ for simulation. Figure 8a shows the result with the 2nd

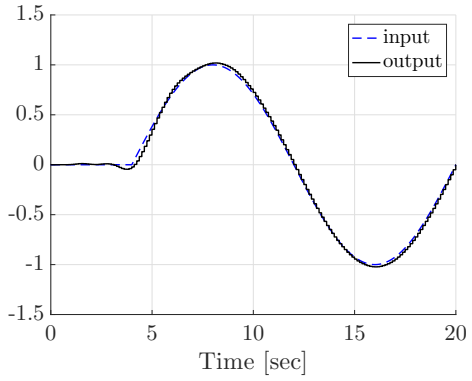

(a) $\sin(\pi/8)t$

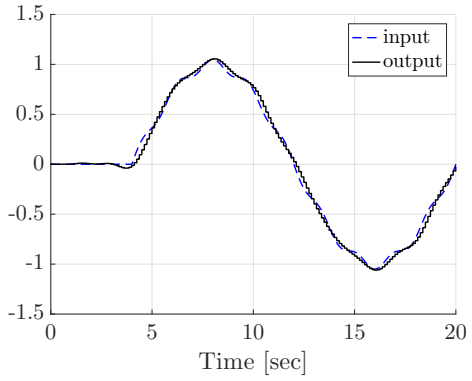

(b) $\sin(\pi/8)t + 0.05\sin(9\pi/8)t$

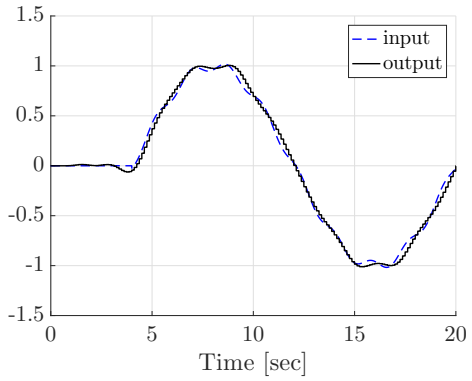

(c) $\sin(\pi/8)t + 0.05\sin((9\pi/8)t + 10)$

Fig. 6: Reconstruction of sinusoids with upsampling factor $M = 8$

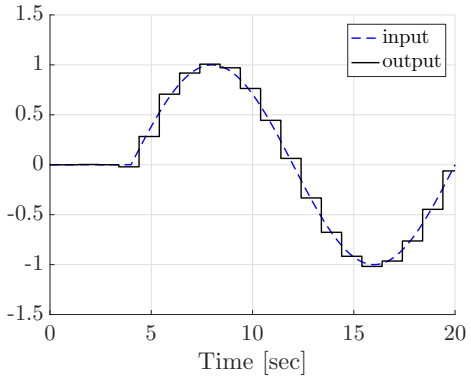

(a) $\sin(\pi/8)t$

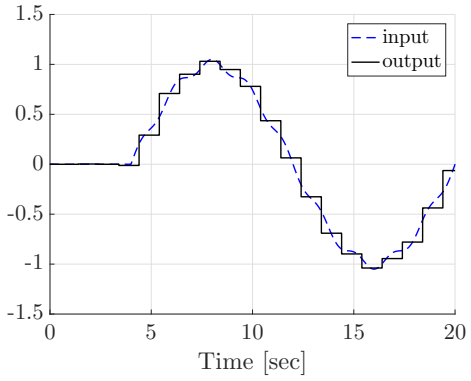

(b) $\sin(\pi/8)t + 0.05\sin(9\pi/8)t$.

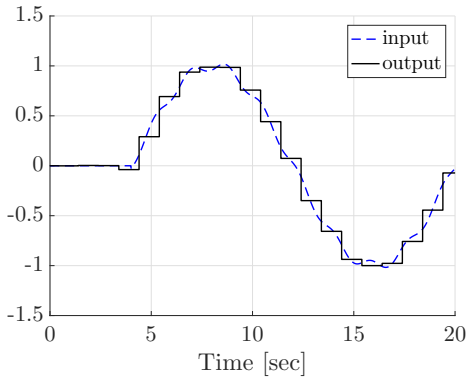

(c) $\sin(\pi/8)t + 0.05\sin((9\pi/8)t + 10)$.

Fig. 7: Reconstruction of sinusoids without upsampling

order Daubechies kernel ${}_2\phi$ while Figure 8b shows the result using a sampled-data filter with ideal sampler by the method developed in [12]. The result by the Daubechies kernel shows larger errors, particularly at discontinuities, which are a result of the continuity of the kernel function, and also of the difference between the ideal sampler and the length of the kernel of this generalized sampler. For comparison, we also show the result by the Haar scaling function in Figure 8c. This shows less ringing than Figure 8a. This is due to the fact that the Haar scaling function has smaller support, and approximates the ideal sampling better.

V. Discussion and Concluding Remarks

We have generalized the sampled-data filter design methodology given in [12] to the more general context involving generalized sampling. This is in conformity with the general situation where sampling is usually associated with a integration with a kernel function, and also with the situation in the wavelet expansion. In particular, we have seen that we can improve the approximation quality by the present method with upsampling. In practice, we do not necessarily have sufficient resolution in the given data, and it is possible to go over to the higher order expansion by optimally interpolating the intersample behavior, and this can

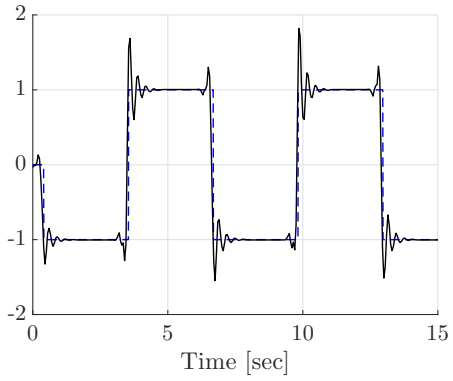

(a) Response against a rectangular wave (Daubechies)

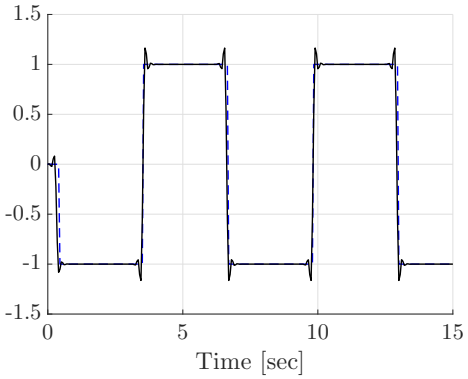

(b) Response via a sampled-data filter with ideal sampler

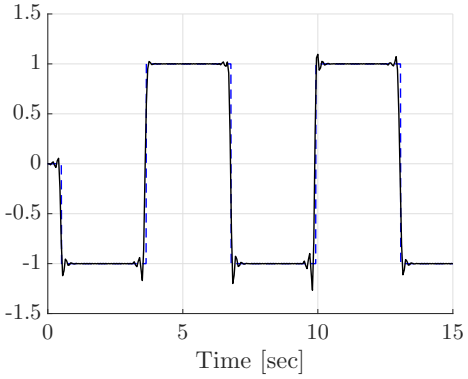

(c) Response via the Haar scaling function

Fig. 8: Response against a rectangular wave

contribute to a higher-order wavelet expansion.

On the other hand, we also note that the performance of the present generalized sampling method with continuous kernels is limited in high frequency as compared to ideal sampling. This performance limitation is in a sense inevitable due to the very nature of generalized sampling that is always accompanied with integration. In this sense, it cannot supersede ideal sampling. The objective of the present study is to generalize the method in [12] for ideal sampling to this generalized context where sampling obeys a more practical constraint. As noted in Examples 4.1 and 4.2, this can be circumvented to some extent as noted above, e.g., as contrasted in Figure 6 vs Figure 7.

To remedy the high frequency performance, one can also resort to expand the residual error via higher-order wavelets, or employ scaling/wavelet functions that are more adequate for high-frequency reconstruction, for example, coiflets or simply Haar scaling function ([2]). However, they cannot outperform ideal sampling as far as the high frequency performance is concerned. This is the consequence of the integration involved in sampling. Some related aspects were discussed in [3], but a more elaborate study is a topic for future study.

We also note that it is possible to extend the present framework to a more general context with *non-orthogonal* scaling functions, in particular, box splines. In such a case, although the scaling functions have compact support, the corresponding expansion cannot be obtained by an inner product with such scaling functions, but rather with their duals. This was discussed partly in [3] as well, but it needs to be explored also in detail in our future study.

REFERENCES

[1] B. Bamieh, J. B. Pearson, B. A. Francis, and A. Tannenbaum, "A lifting technique for linear periodic systems with applications to sampled-data control," *Syst. Control Lett.*, vol. 17, no. 2, pp. 79–88, 1991.

[2] I. Daubechies, *Ten Lectures on Wavelets*. Philadelphia: SIAM, 1992.

[3] K. Kashima, Y. Yamamoto, and M. Nagahara, "Optimal wavelet expansion via sampled-data control theory," *IEEE Signal Processing Lett.*, vol. 11, no. 2, pp. 89–82, 2004.

[4] M. Nagahara and Y. Yamamoto, "Frequency domain min-max optimization of noise-shaping delta-sigma modulators," *IEEE Trans. Signal Processing*, vol. 60, no. 6, pp. 2828–2839, 2012.

[5] ——, "H^∞-optimal fractional delay filters," *IEEE Trans. Signal Processing*, vol. 61, no. 18, pp. 4473–4480, 2013.

[6] C. E. Shannon, "Communication in the presence of noise," *Proc. IRE*, vol. 38, pp. 10–21, 1949.

[7] G. Strang and T. Nguyen, *Wavelets and Filter Banks*. Wellesley, Massachusetts: Wellesley-Cambridge Press, 1996.

[8] Y. Yamamoto, "Digital/analog converters and a design method for the pertinent filters," *Japanese patent No. 3820331*, 2006.

[9] ——, "A function space approach to sampled-data control systems and tracking problems," *IEEE Trans. Autom. Control*, vol. AC-39, no. 4, pp. 703–713, 1994.

[10] Y. Yamamoto and P. P. Khargonekar, "Frequency response of sampled-data systems," *IEEE Trans. Autom. Control*, vol. AC-41, no. 2, pp. 166–176, 1996.

[11] Y. Yamamoto and M. Nagahara, "Sample-rate converters," *Japanese patent No. 3851757*, 2006.

[12] Y. Yamamoto, M. Nagahara, and P. P. Khargonekar, "Signal reconstruction via H^∞ sampled-data control theory—beyond the Shannon paradigm," *IEEE Trans. Signal Processing*, vol. SP-60, no. 2, pp. 613–625, 2012.

[13] A. I. Zayed, *Advances in Shannon's Sampling Theory*. CRC Press, Boca Raton, 1993.